NATIONAL ADVISORY COMMITTEE FOR AERONAUTICS

REPORT No. 229

PRESSURE DISTRIBUTION OVER THICK TAPERED AIRFOILS, N. A. C. A. 81, U. S. A. 27 C MODIFIED AND U. S. A. 35

By ELLIOTT G. REID

WASHINGTON
GOVERNMENT PRINTING OFFICE
1926

AERONAUTICAL SYMBOLS

1. FUNDAMENTAL AND DERIVED UNITS

	Symbol	Metric		English	
		Unit	Symbol	Unit	Symbol
Length	l	meter	m	foot (or mile)	ft. (or mi.).
Time	t	second	sec	second (or hour)	sec. (or hr.).
Force	F	weight of one kilogram	kg	weight of one pound	lb.
Power	P	kg/m/sec		horsepower	HP.
Speed		m/sec		mi./hr	M. P. H.

2. GENERAL SYMBOLS, ETC.

Weight, $W=mg$.

Standard acceleration of gravity, $g=9.80665\text{m/sec}^2=32.1740\text{ft./sec.}^2$

Mass, $m=\frac{W}{g}$

Density (mass per unit volume), ρ

Standard density of dry air, 0.12497 (kg-m^{-4}-sec^2) at 15°C and 760 mm = 0.002378 (lb.-ft.$^{-4}$-sec.^{2})

Specific weight of "standard" air, 1.2255 kg/m^3 = 0.07651 lb./ft.^{3}

Moment of inertia, mk^2 (indicate axis of the radius of gyration, k, by proper subscript)

Area, S; wing area, S_w, etc.

Gap, G.

Span, b; chord length, c.

Aspect ratio $=b/c$.

Distance from $c.\ g.$ to elevator hinge, f.

Coefficient of viscosity, μ.

3. AERODYNAMICAL SYMBOLS

True airspeed, V.

Dynamic (or impact) pressure, $q=\frac{1}{2}\rho V^2$

Lift, L; absolute coefficient $C_L=\frac{L}{qS}$

Drag, D; absolute coefficient $C_D=\frac{D}{qS}$

Cross-wind force, C; absolute coefficient $C_c=\frac{C}{qS}$

Resultant force, R.

(Note that these coefficients are twice as large as the old coefficients L_c, D_c.)

Angle of setting of wings (relative to thrust line), i_w.

Angle of stabilizer setting with reference to thrust line, i_t.

Dihedral angle, γ.

Reynolds Number $=\rho\frac{Vl}{\mu}$ where l is a linear dimension.

e. g., for a model airfoil 3 in. chord, 100 mi./hr., normal pressure, 0°C: 255,000 and at 15°C, 230,000;

or for a model of 10 cm chord, 40 m/sec, corresponding numbers are 299,000 and 270,000.

Center of pressure coefficient (ratio of distance of $C.\ P.$ from leading edge to chord length), C_p.

Angle of stabilizer setting with reference to lower wing. $(i_t-i_w)=\beta$.

Angle of attack, α.

Angle of downwash, ϵ.

REPORT No. 229

PRESSURE DISTRIBUTION OVER THICK TAPERED AIRFOILS, N. A. C. A. 81, U. S. A. 27 C MODIFIED AND U. S. A. 35

By ELLIOTT G. REID
Langley Memorial Aeronautical Laboratory

52767—26†——1

ADDITIONAL COPIES
OF THIS PUBLICATION MAY BE PROCURED FROM
THE SUPERINTENDENT OF DOCUMENTS
GOVERNMENT PRINTING OFFICE
WASHINGTON, D. C.
AT
10 CENTS PER COPY

REPORT No. 229

PRESSURE DISTRIBUTION OVER THICK TAPERED AIRFOILS, N. A. C. A. 81, U. S. A. 27 C MODIFIED, AND U. S. A. 35

By Elliott G. Reid

SUMMARY

At the request of the United States Army Air Service, the tests reported herein were conducted in the 5-foot atmospheric wind tunnel of the Langley Memorial Aeronautical Laboratory. The object was the measurement of pressures over three representative thick, tapered airfoils which are being used on existing or forthcoming Army airplanes. The results are presented in the form of pressure maps, cross-span load and normal force coefficient curves and load contours.

The pressure distribution along the chord was found very similar to that for thin wings, but with a tendency toward greater negative pressures. The characteristics of the loading across the span of the U. S. A. 27 C modified are inferior to those of the other two wings; in the latter, the distribution is almost exactly elliptical throughout the usual range of flying angles.

The form of tip incorporated in these models is not completely satisfactory and a modification is recommended.

INTRODUCTION

In the light of recent studies of accelerations in flight and some unexpected structural failures in the air, the schedule of required load factors for Army airplanes has been made much more severe than that formerly used. Consequently the design of wing cellules and the proper loading of wings in static test have become more serious problems than ever before. This is particularly true of pure or semi cantilever construction which involves the use of thick, tapered wings.

Determinations of the magnitude and disposition of the air loads imposed upon representative wings of this type have therefore been carried out.

METHODS AND APPARATUS

The pressure distribution measurements described below were made on half-span models of the following airfoils: N. A. C. A. 81, U. S. A. 27 C modified, and U. S. A. 35. The first is a double convex section of small mean camber; it is linearly tapered both in thickness and plan form. The second is also doubly convex but of larger camber; it is of constant section for about a chord length at midspan and is tapered linearly in plan form and thickness from this section to a tip which is washed out 1.5 degrees. The third airfoil has a slightly concave lower surface and the greatest camber of the group; its taper is linear in plan form and thickness.

Models.—The models were built of mahogany laminations and inlaid with soft brass tubes of 0.050 inch (1.27 millimeters) outside diameter. The N. A. C. A. 81 and a sample lamination are shown in Figure 1. Details of the models, location of orifices, etc., are given in Figures 2, 3, and 4.

Into each model were built between 70 and 80 tubes which had their open ends distributed along the 6 chosen chords of the semispan. The portion of each lamination to be included within the finished model was laid out and the tube grooves made within these limits. Tubes were then cut to extend slightly beyond the model surface and well beyond the wing butt. Glue and dowel pins were used to build up the laminations into complete wing blanks.

Models were cut to shape entirely by hand. Templates were fitted at the ends of the tapered sections and a straightedge used to check the surface between proportional chord stations.

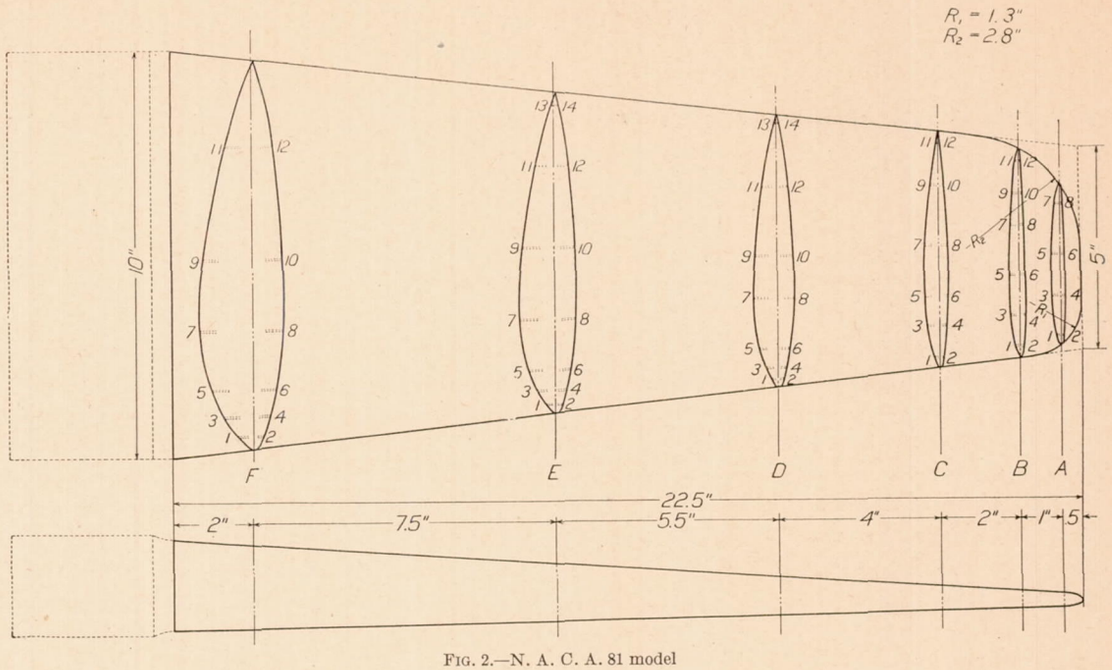

FIG. 2.—N. A. C. A. 81 model

The tip form adopted was one designed to allow the use of two spars of approximately equal length and yet realize the aerodynamic advantages common to elliptical and negatively

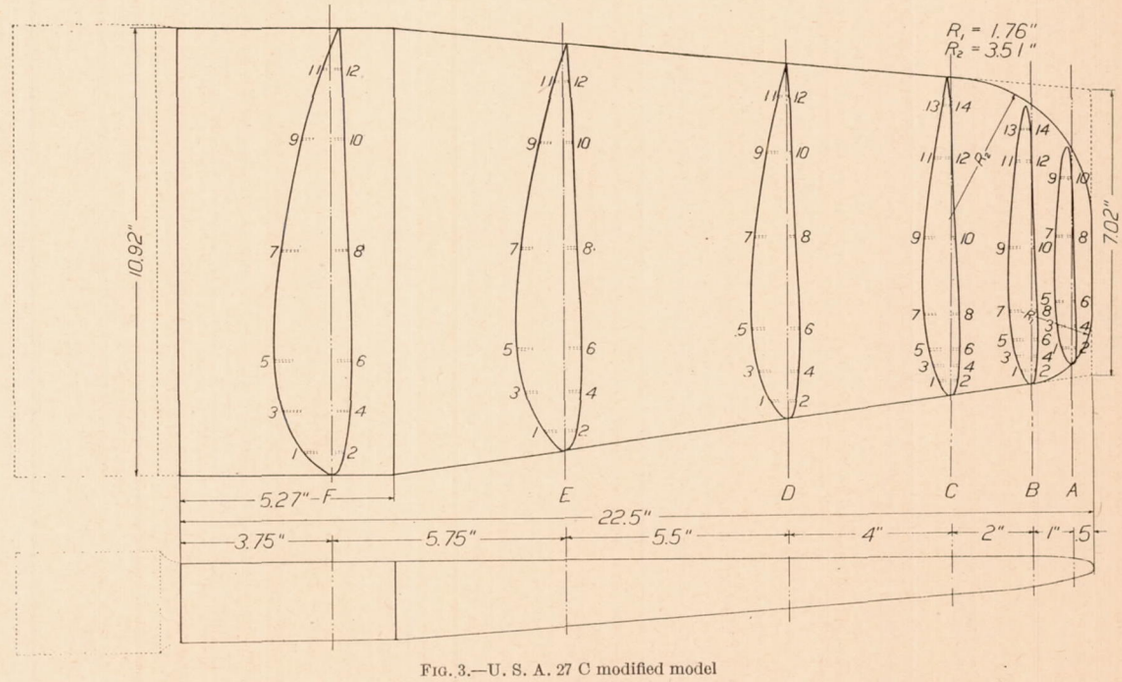

FIG. 3.—U. S. A. 27 C modified model

raked tips. To incorporate this modified tip, the model was first finished in the original trapezoidal plan form, the ordinates at tip and root being those given in Table I. The corners were then removed to give the desired plan form, a "mean camber line" scribed around the

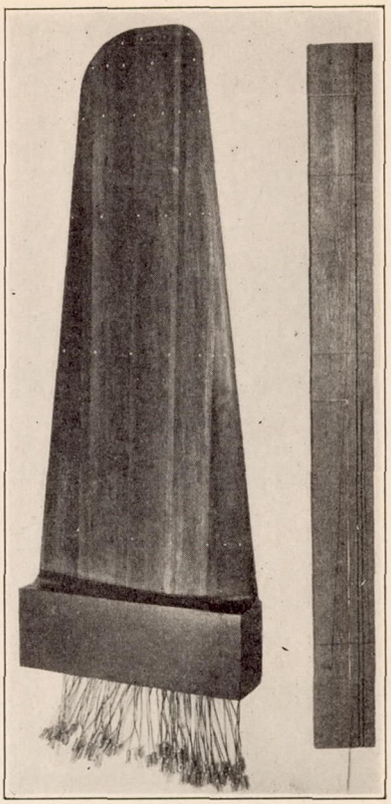

FIG. 1.—N. A. C. A. 81 model and sample lamination with tube in place

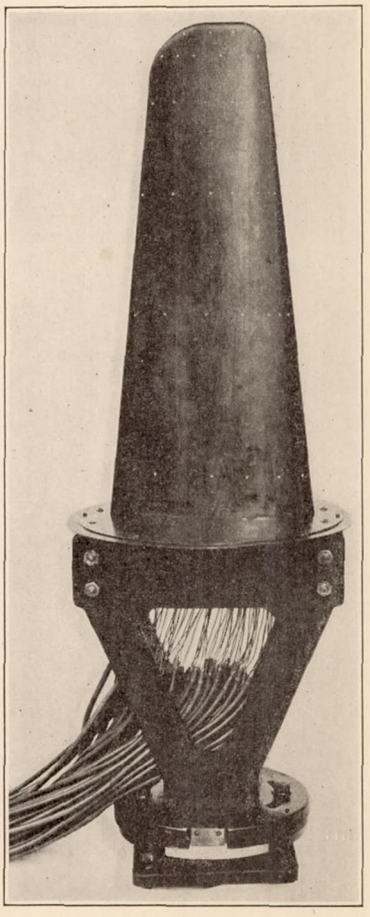

FIG. 5.—Model assembled in supporting pedestal

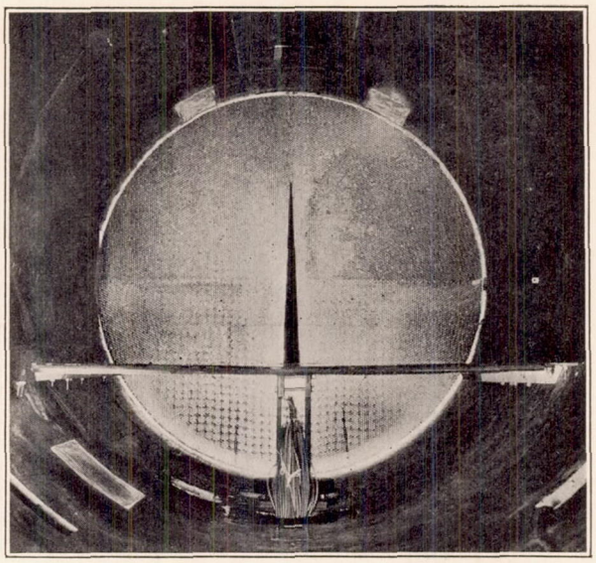

FIG. 6.—View upstream in tunnel before inclosing pedestal

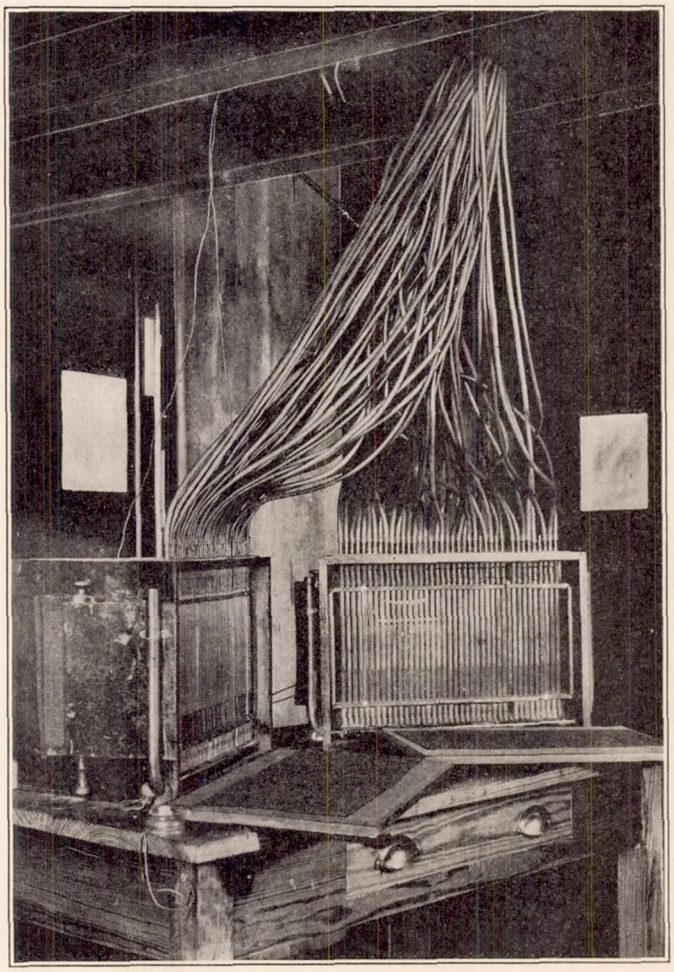

FIG. 7.—Manometer installation

square tip, and the surface faired down to this line. A form approximating that of the leading edge was maintained well around the front corner; the radius was then gradually reduced to give a smooth transition into the sharp trailing edge. The resulting multilations of the original surface extended inward to a maximum distance of 10–15 per cent of the original tip chord; the actual contours of the sections close to the tip were obtained from plaster casts taken after completion of the tests and are represented, to true scale, in Figures 2, 3, and 4.

Apparatus.—The models were supported in a heavy cast-iron pedestal, or bracket, which could be rotated on a base affixed to the bottom of the tunnel. A sheet-metal "plane of symmetry," which extended clear across the tunnel, was used to replace, in effect, the other half of the wing by its reflecting or "mirror" action.

Out of this plane was cut a disk and a disk of very slightly smaller diameter was fitted to the wing and carried on bosses on the supporting bracket, as shown in Figure 5. The small gap between disk and plane was sealed by a sheet-metal ring attached to the under side of the disk. The reflecting plane extended 38.5 inches (978 millimeters) upstream and 40.5 inches

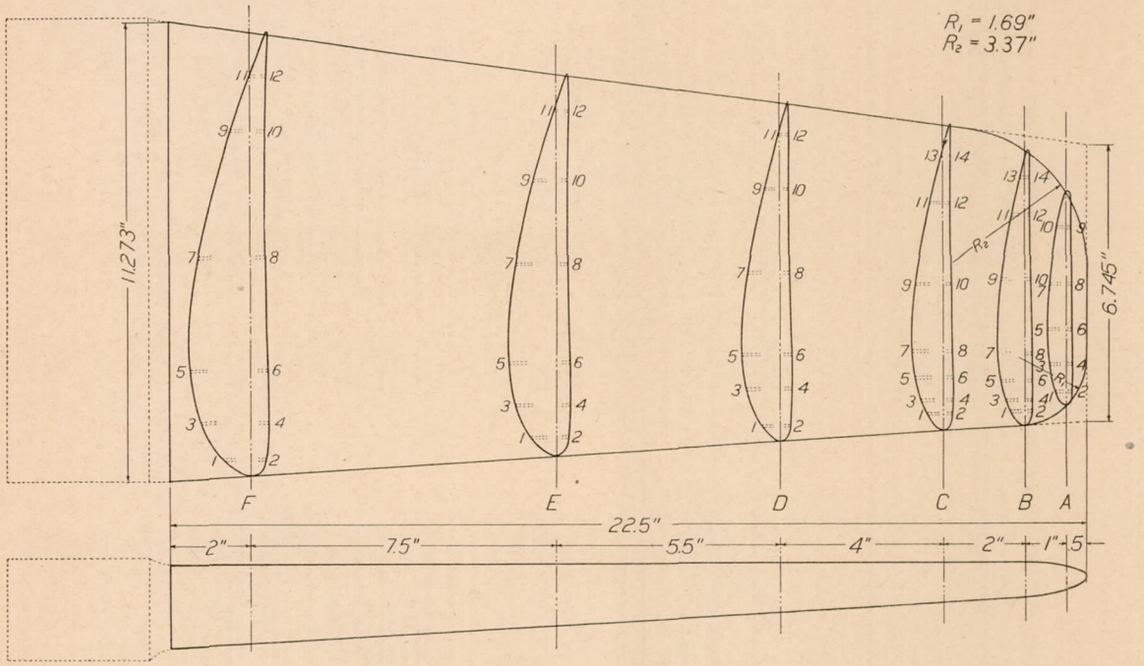

FIG. 4.—U. S. A. 35 model

(1,030 millimeters) downstream from the axis of the supporting bracket. The installation is shown in Figure 6; this photograph is incomplete as a fixed, sheet-metal streamline entirely enclosed the bracket and tubes during testing. It will be noted that wing tip and dividing plane are equidistant, respectively, from top and bottom of the tunnel.

Rubber tubes were led from the wing butt to the two recording multiple manometers which were placed on a table directly below the model (see fig. 7). All upper surface tubes were connected to one manometer and lowers to the other; tubes from adjacent stations were connected to corresponding manometer tubes so that pressure maps could be observed directly in the manometers. This arrangement was very convenient in the location of the angles of attack of zero and maximum normal force. The end tubes of each manometer were connected to a static orifice on the tunnel wall above and just forward of the wing tip. This pressure was used as the reference from which positive and negative pressures were measured.

Small electric bulbs in the backs of the manometers furnished the illumination for exposure of the record blanks of sensitized paper. Blanks were held in contact with the tubes so that direct prints were made, thus eliminating any scaling factor. A sample record is shown in Figure 8.

Procedure.—Before any records were taken, a velocity survey was made directly in front of the model. It was found that the velocity close to the plane was considerably higher than that in the free stream above it. This was quite evidently due to the restriction of the flow beneath the plane by the large stream line required to enclose the bracket.

To remedy this condition, the leading edge of the reflecting plane was slightly elevated. A new velocity survey showed an improved condition and by a series of trials a position giving a very uniform velocity distribution across the span was found. All these preliminary trials were made with the wing at approximately the angle of zero normal force. A satisfactory distribution having been found for this condition, the wing was turned to a large angle and another survey made. To eliminate possible yaw effects on the exploring Pitot, the instrument was turned to parallelism with a silk thread held just above its nose.

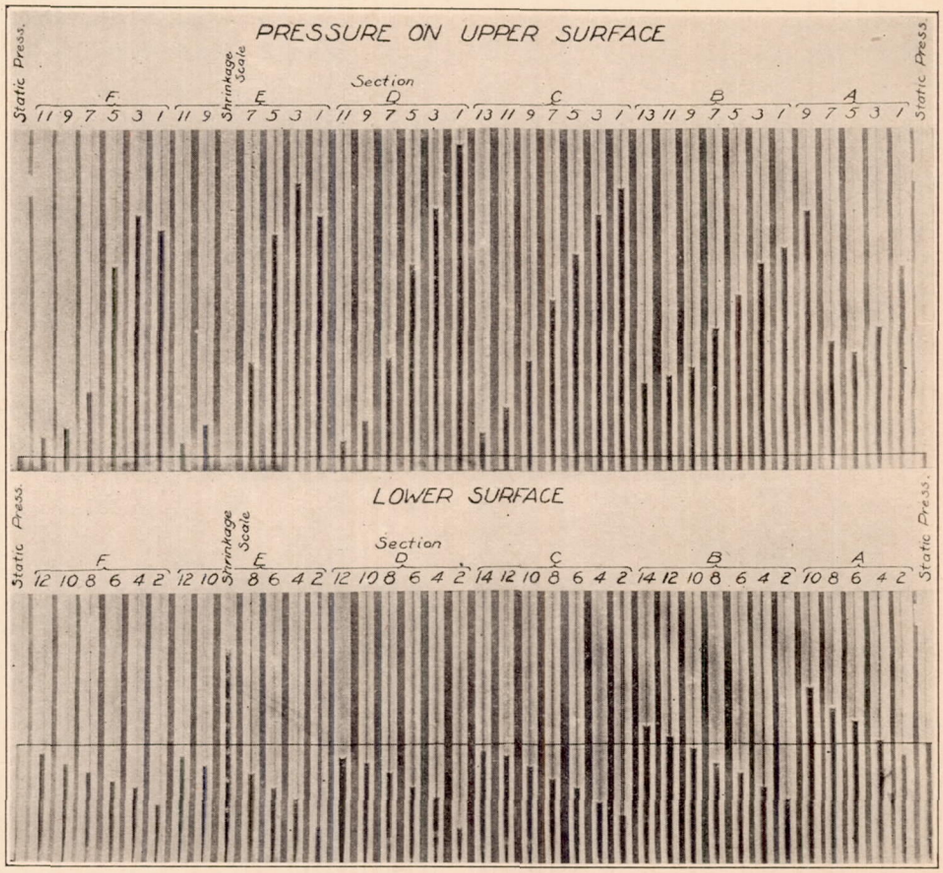

FIG. 8.—Sample manometer record

Results of the two velocity surveys, for the final position of the leading edge of the plane, are given in Figure 9. The dynamic head used in computations was the average of the integrated means of these values. (In the integration, only values between a point 2 inches (50.8 millimeters) above the plane and the wing tip were used.)

Following the establishment of a satisfactory velocity distribution, preliminary runs were made to determine the range of angles to be covered and to make sure that the pressures encountered were within the range of the manometers.

It was found possible to test two of the models at 25 m/s (82.0 ft./s.) but the negative pressures on the U. S. A. 35 were so large that the speed had to be reduced to 22.5 m/s (73.9 ft./s.).

During the taking of records, air speed was maintained constant according to the regular "service Pitots," which is located upstream from the fine honeycomb marking the forward end of the straight throat section of the tunnel.

The actual taking of records was a very short, direct process. The angle of attack was set by means of a vernier on the supporting bracket, the air speed adjusted to the proper value, and the manometers loaded. A few seconds were allowed to elapse for the establishment of steady conditions and then an exposure of about one-half second was made.

Accuracy.—Models were constructed to a maximum tolerance of one-tenth of 1 per cent of the average chord.

After connection with the manometers, each line was checked for leakage and sluggishness. During the tests there were no fluctuations of liquid level sufficiently large or rapid to give indistinct records. The consistency of the method was proved by repeating a run at a high angle of attack several days after the original had been made. Areas of the pressure maps from the two runs were imperceptibly different.

Records were carefully scaled for possible shrinkage of the paper but this was found to be negligible. Planimetering of the pressure maps was held well within an accuracy of 1 per cent except in the smallest diagrams. The faring of curves was susceptible to errors of possibly 2 to 3 per cent. It seems probable that the final curves are accurate to within ± 2 per cent.

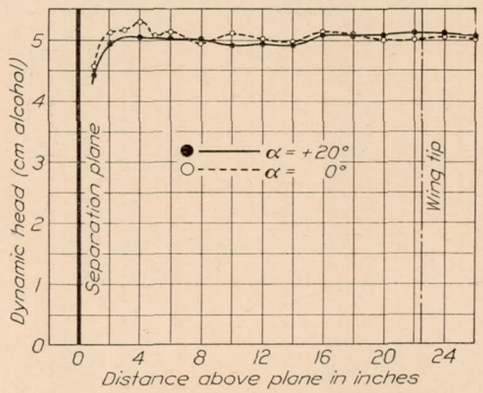

FIG. 9.—Velocity survey above separation plane

ADVANTAGES OF THE METHOD

The present method has three important advantages over those previously used in airfoil pressure distribution work. They are: Attainment of large Vl product by use of large models, elimination of the interference effects of supporting apparatus and pressure leads, and uniformity of results through simultaneous recording of pressures at all points of the wing's surface.

The question of tunnel wall interference might be of large importance, with models of the present size, if we were concerned with drag. However, the effect of drag variation upon normal force is small. If any serious effect upon the "apparent aspect ratio" were present, one would expect to find a considerable difference between the slopes of the curves of normal force versus angle of attack for these large models and for small ones. This does not seem to be the case.

Measurements of pressure taken very close to the dividing plane might be open to criticism as we know that there is a very sharp reduction of velocity in this region. The results obtained for loading across the span, however, seem to be altogether consistent and it is concluded that the closest station was sufficiently removed from the dividing plane to escape this influence.

RESULTS AND DISCUSSION

Pressure maps for the individual stations along the span are given in Figure 10 for the N. A. C. A. 81, in Figure 11 for the U. S. A. 27 C modified, and in Figure 12 for the U. S. A. 35. The contour charts, Figures 13 to 15, were made directly from these maps and represent the total pressure differences between upper and lower surfaces.

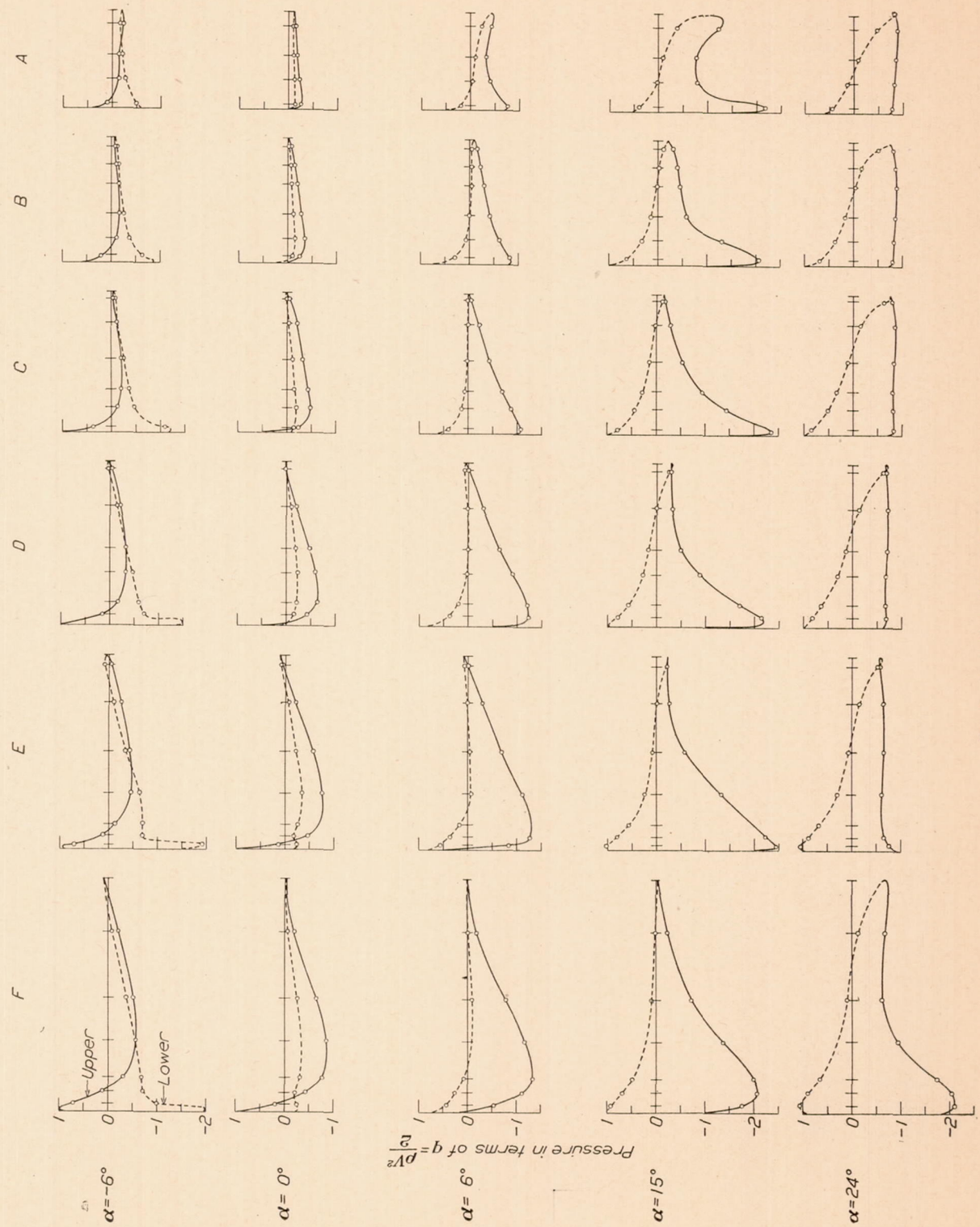

FIG. 10.—N. A. C. A. 81 pressure maps

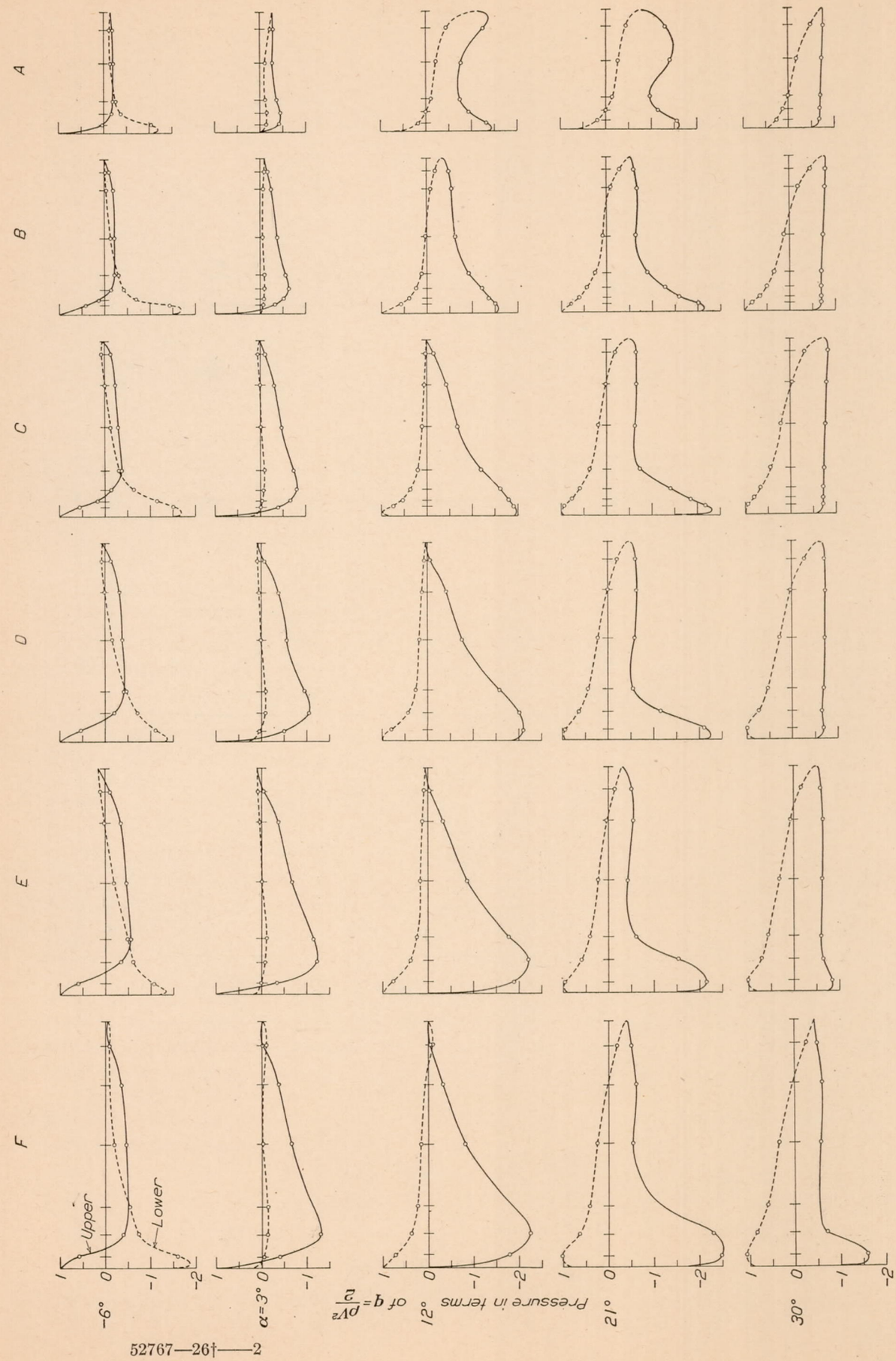

FIG. 11.—U. S. A. 27 C modified pressure maps

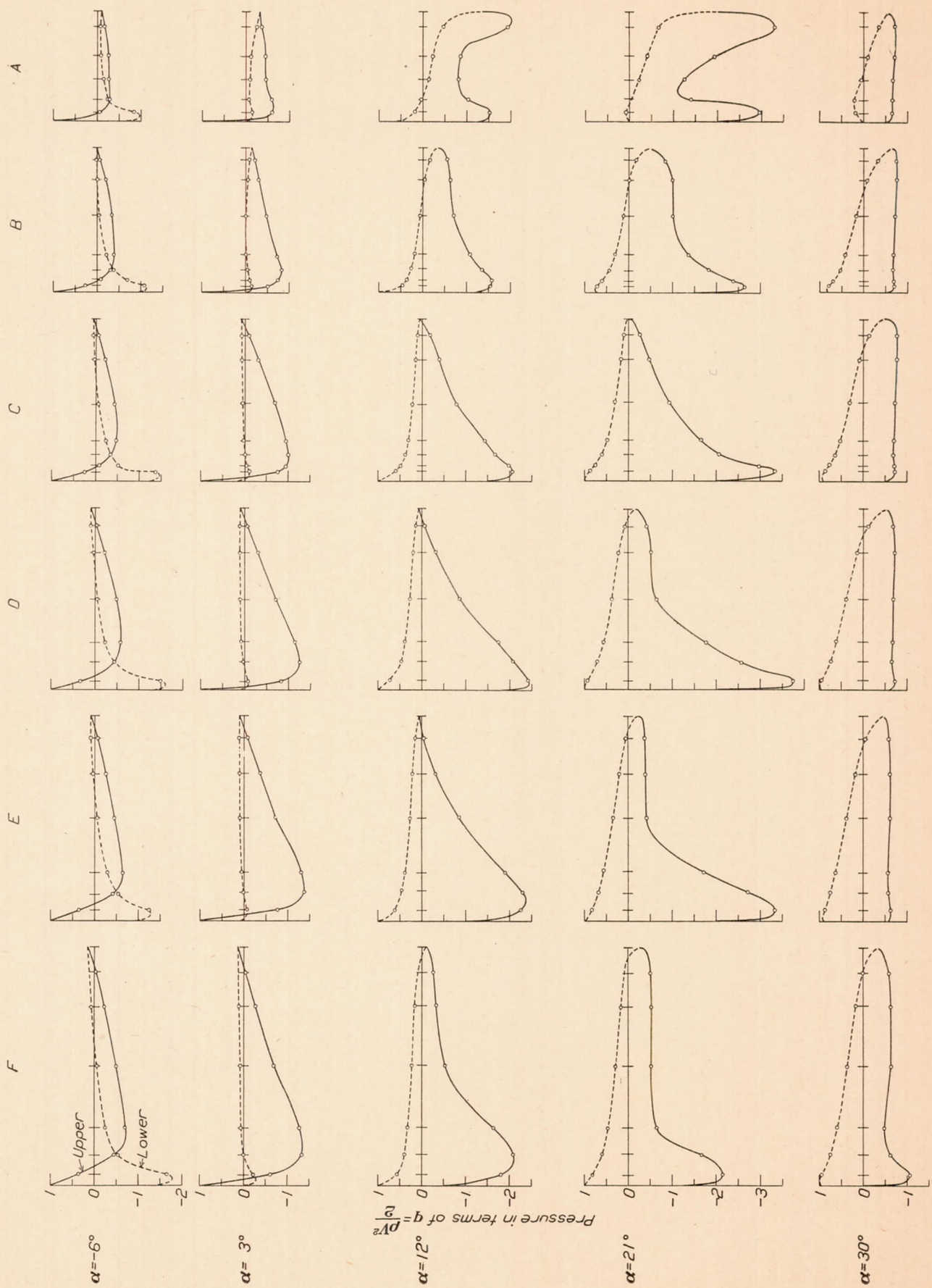

FIG. 12.—U. S. A. 35 pressure maps

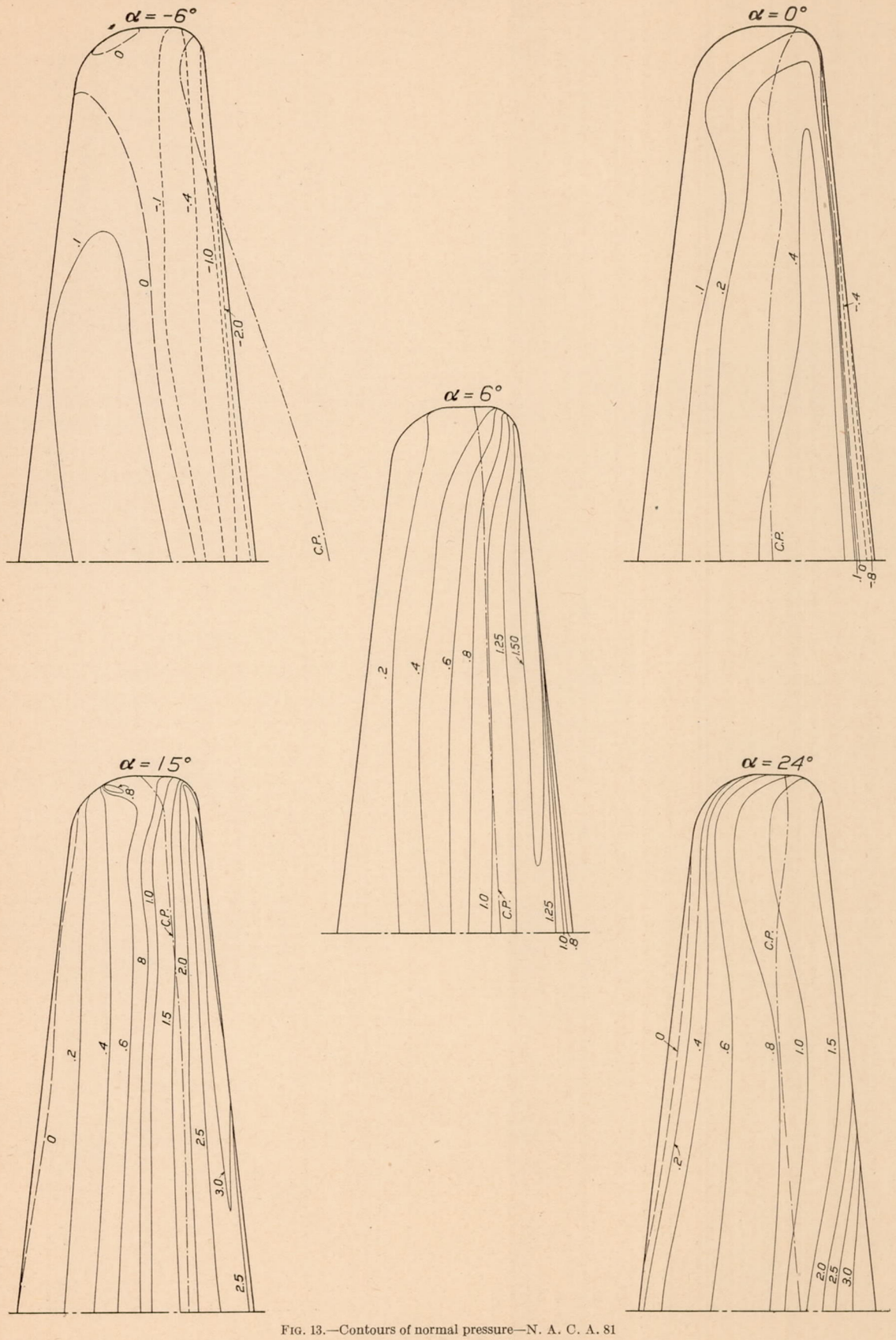

FIG. 13.—Contours of normal pressure—N. A. C. A. 81

(In terms of $q=\frac{\rho V^2}{2}$)

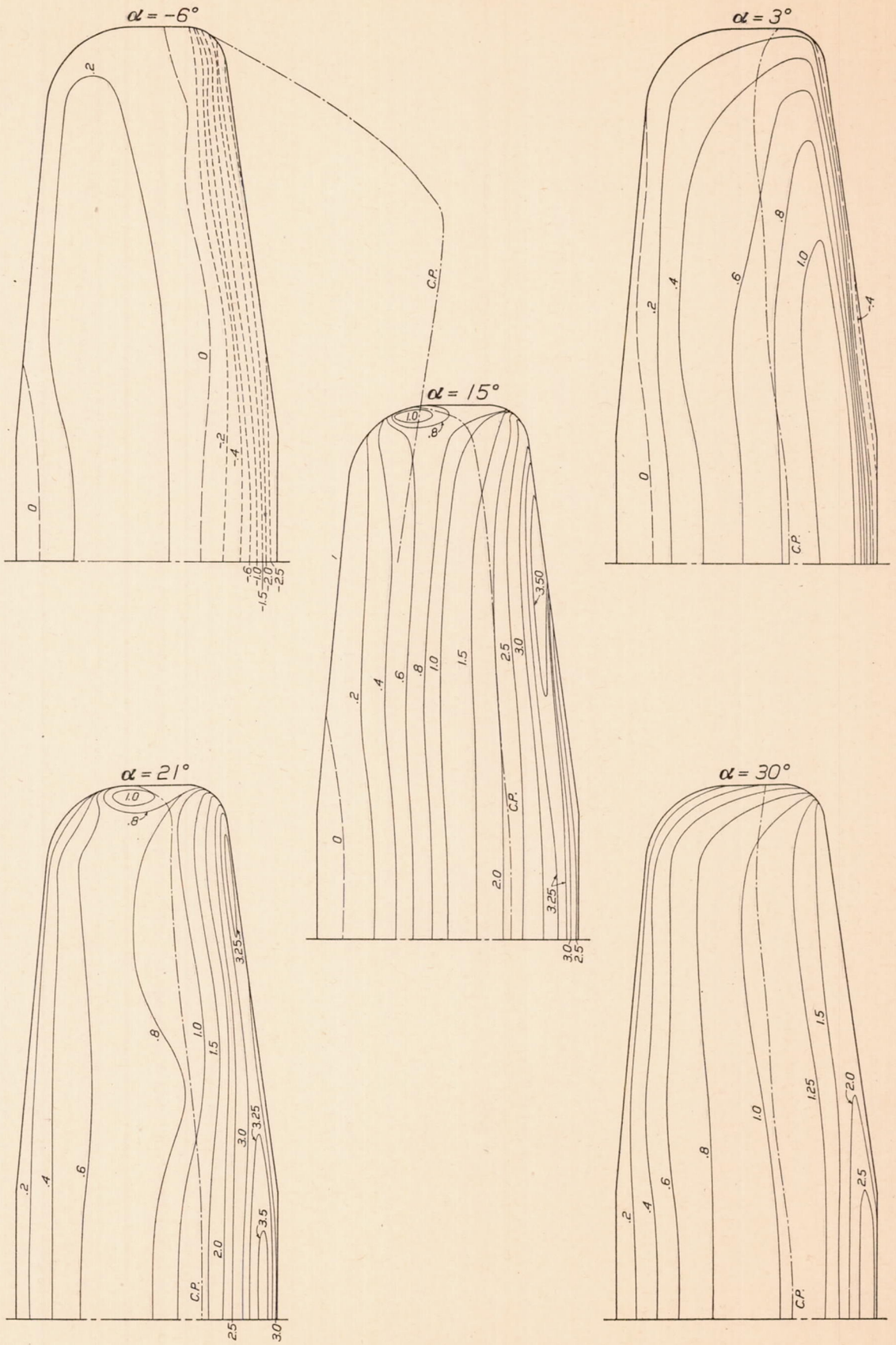

FIG. 14.—Contours of normal pressure—U. S. A. 27 C modified
(In terms of $q = \frac{\rho V^2}{2}$)

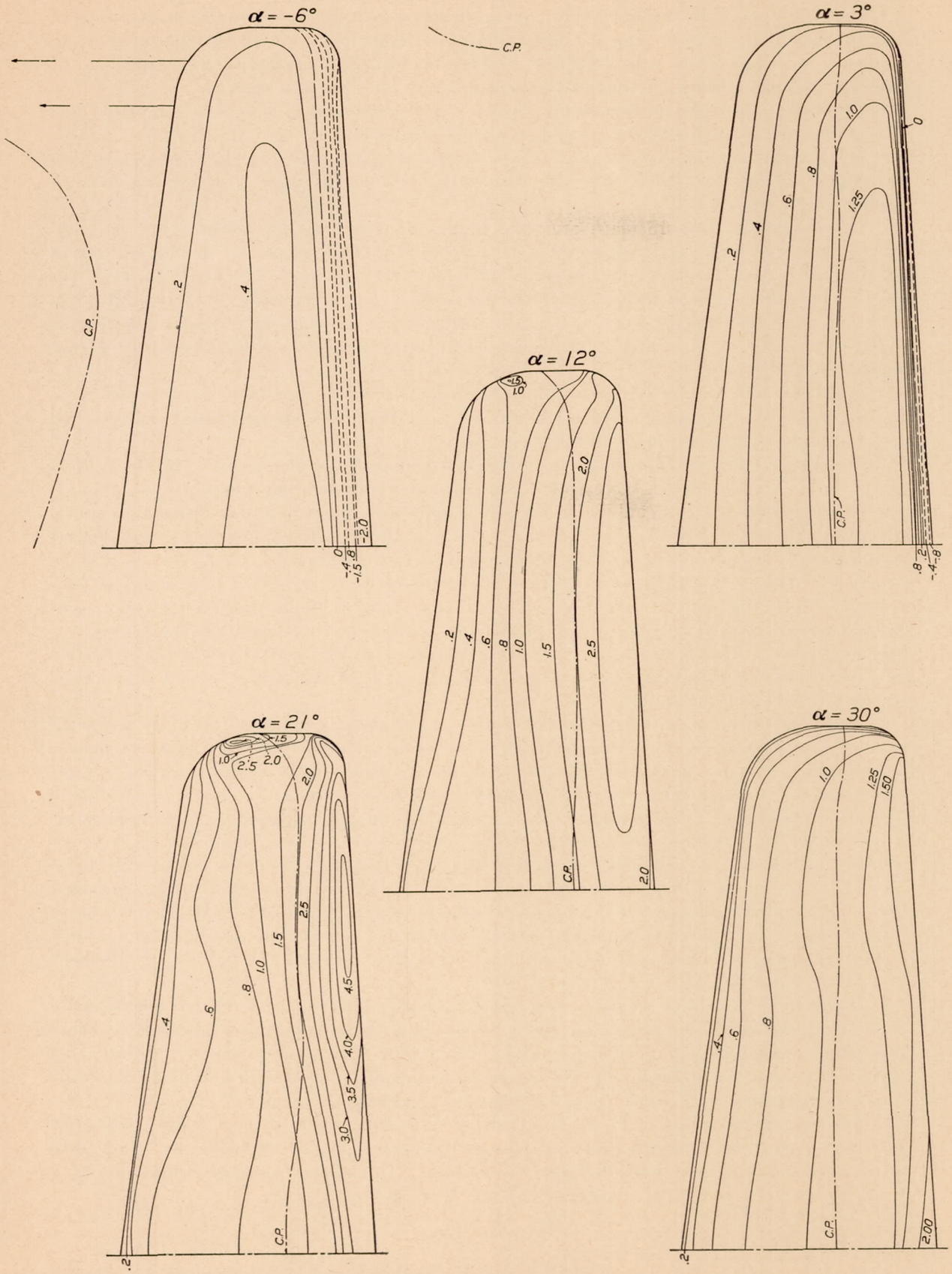

FIG. 15.—Contours of normal pressure—U. S. A. 35

(In terms of $q=\frac{\rho V^2}{2}$)

The load curves, Figures 16 to 18, have ordinates which are proportional to the areas of the corresponding pressure maps; a nondimensional ordinate has been introduced to avoid confusion in computations involving the varying chord. The coefficient K is equal to C_N times (chord/span); hence, K times q times span equals load per unit span.

From each load, the corresponding normal force coefficient C_N has been calculated and these values are plotted against the span as Figures 19, 20, and 21.

The areas under these curves have been integrated and divided by the semispan to give the values of C_N for the whole wing; the final plots of C_N versus angle of attack are given in Figures 22, 23 and 24.

The individual pressure maps are very similar to those for thin wings. The one outstanding effect of large thickness seems to be a depression of the front and middle portions of the diagrams, i. e., for the same pressure difference between upper and lower surfaces, the absolute pressures on both surfaces are lower for a thick than a thin wing. As zero lift is approached, this effect appears as a downward tilting of the pressure map toward the leading edge. Convexity of the lower surface accentuates this condition very noticeably, as was pointed out in Reference 2.

In general, the loading across the span on all three airfoils is satisfactory. The two main objectives of obtaining small moments about the spar roots and approximately elliptical lift distribution have been attained in all three wings.

Through the angles of the usual flying range, the loadings across the spans of the N. A. C. A. 81 and U. S. A. 35 approach the elliptic form very closely. From this point of view, there is little choice between them, unless it is that the moments about the spar roots are slightly greater for the latter. The load curves for the U. S. A. 27 C modified, however, droop toward midspan and consequently make this airfoil inferior to the other two.

In the high speed or diving range, the inferiority of the U. S. A. 27 C modified is very marked. From the load curves it may be seen that at zero lift the loading changes sign twice in the semispan, that is, there is positive lift at the quarter span point and negative lift at the tips and center. This would stress the spars excessively at the quarter points and probably give rise to uncertain stability and tricky control in a dive, as the airflow in such a condition is bound to be highly unstable.

It will be seen that on both the other wings, to obtain zero lift over the whole wing, the tip must be at negative lift. The condition indicates an excessive washout. Though neither of these wings has any "geometric washout," the aerodynamic characteristic is present to quite a large degree; the washout referred to here is the difference between the angles of zero lift of root and tip sections. This is considered an undesirable quality, particularly in its application to cantilever construction. It could easily be remedied by the use of a slight geometric washin which should not seriously detract from the good characteristics of the positive lift range.

The distribution of load at maximum lift is of considerable importance in the consideration of accelerated flight and, for this reason, the lateral centers of pressure have been calculated from the load curves for this condition. They were found to lie at the following percentages of the semispan, as measured from the center: N. A. C. A. 81, 41.9; U. S. A. 27 C modified, 44.3; U. S. A. 35, 45.5.

It will be noticed that while the sections midway between root and tip burble first in the N. A. C. A. 81 and U. S. A. 27 C modified, the U. S. A. 35 behaves quite differently. When this airfoil reaches maximum lift, the loads at the center of the span begin to decrease, then there is a more or less uniform reduction across the entire span and this is followed by an abrupt drop which attains its greatest value at about the quarter-span point.

The maximum intensity of load found along the leading edges of these wings would indicate that shape of the forward portion of the airfoil is more important than camber, for the order of maxima does not agree with the order of cambers. The highest loads recorded were N. A. C. A. 81, 4.0 q; U. S. A. 27 C modified, 3.5 q; and U. S. A. 35, 4.7 q.

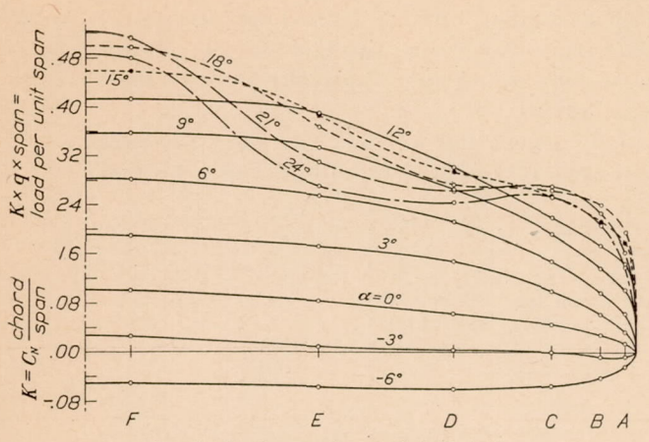

FIG. 16.—Loads on semi-span; N. A. C. A. 81

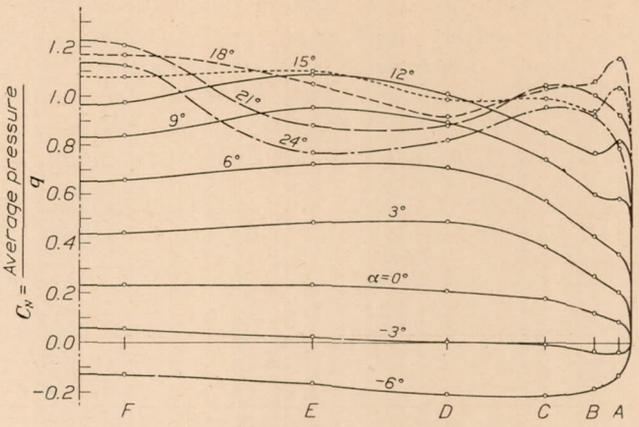

FIG. 19.—Normal force coefficients—N. A. C. A. 81

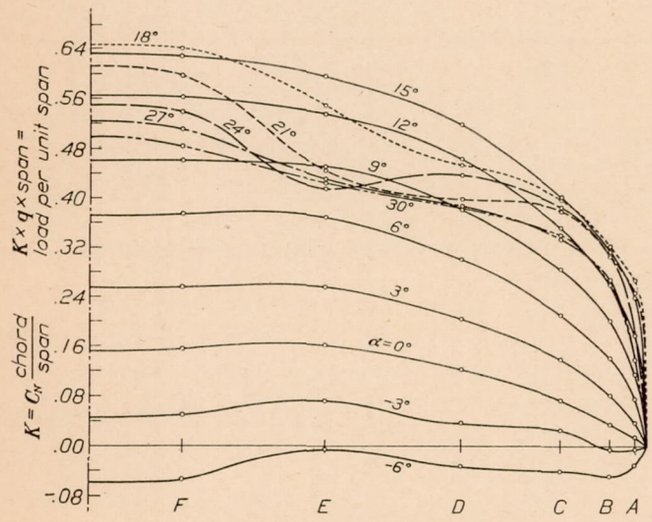

FIG. 17.—Loads on semi-span; U. S. A. 27 C modified

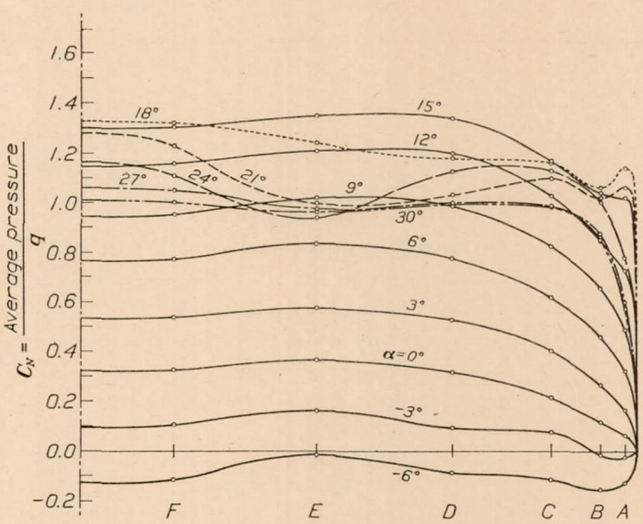

FIG. 20.—Normal force coefficients—U. S. A. 27 C modified

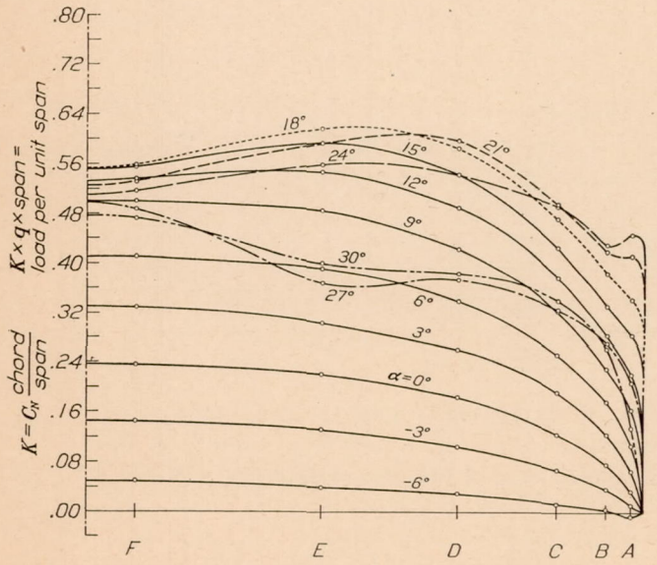

FIG. 18.—Loads on semi-span; U. S. A. 35

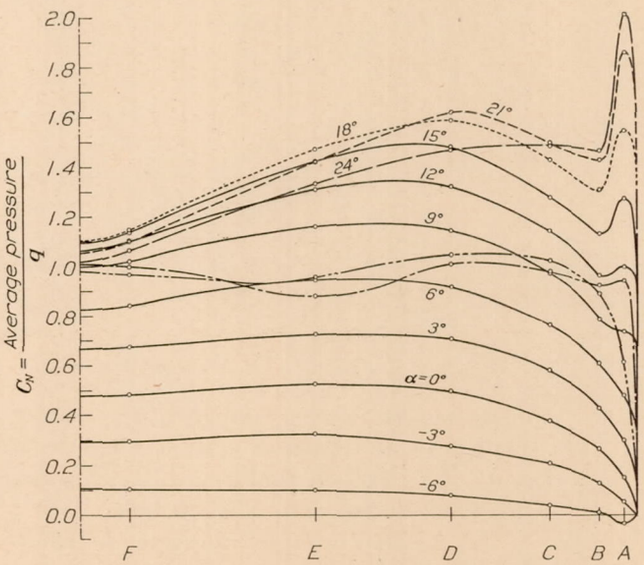

FIG. 21.—Normal force coefficients —U.S. A. 35

The pressures over the tips of these airfoils are of particular interest from both structural and aerodynamic standpoints. It was hoped, when this plan form was laid out, to obtain contours somewhat approximating those of the negatively raked and elliptically tipped wings. The contours show that the results fell short of expectations.

On the N. A. C. A. 81, the tip loading is not really severe, but a small secondary pressure peak does appear at high lifts. This high local pressure is forward of the limits of a normal

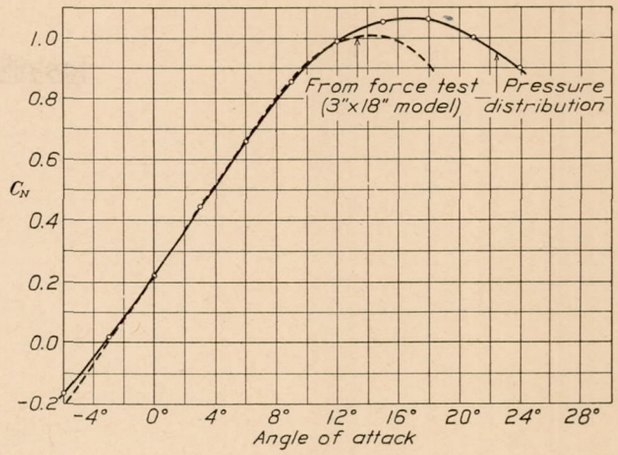

FIG. 22.—Total normal force—N. A. C. A. 81

aileron but might move easily back onto the aileron if the surface were given a large down angle. The maximum load found in the secondary peak has an intensity of 0.8 q. The condition on the U. S. A. 27 C modified was similar to that of the N. A. C. A. 81, reaching a maximum value of 1.0 q and having approximately the same location.

In the case of the higher cambered *U. S. A. 35*, however, this secondary peak reached alarming proportions. Its maximum intensity was 2.6 q and it extended so far forward as to nearly

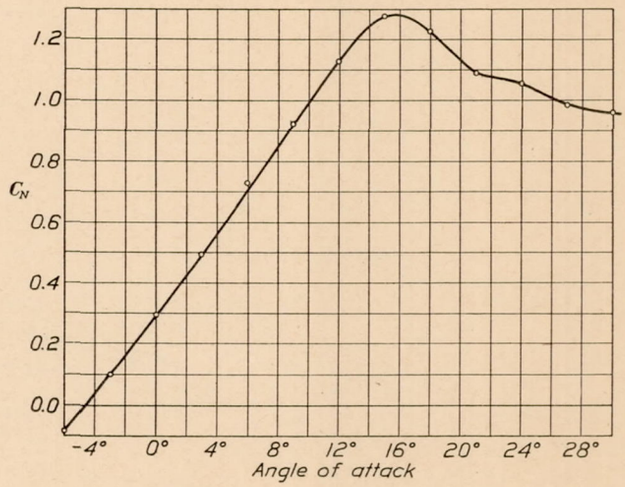

FIG. 23.—Total normal force—U. S. A. 27 C modified

join the high pressure region along the leading edge. The cross-span load curve actually shows a small peak at the outer station whereas the curves for the other wings drop rapidly in this region. It is certain that operation of a normal aileron would not be satisfactory with a tip of this kind on the U. S. A. 35 airfoil.

The peculiar form of pressure distribution found on these tips seems to demand some explanation. The contours resemble both those for rectangular and elliptical tips (Reference 1)

in some details. The high pressure region along the leading edge swings back, as on the elliptical tip, and the secondary peak appears as in the rectangular one. Almost the same condition will be found on the wing No. 59, previously tested. (Reference 2.) It is thought that if this wing had been tested at the angle of maximum lift, the secondary peak would have been even higher than that on the U. S. A. 35 because of its greater camber. It appears that the reduction of chord close to the wing tip plays a part nearly as important as does the distribution of area with respect to the leading edge. The shape of tip used in these tests gives less reduction of chord close to the tip than do the elliptical or raked tips shown in Reference 1, and the close resemblance to the rectangular tip is blamed for the unsatisfactory distribution. In Figure 25, chord is plotted against span for the three shapes of tip; the curve for a suggested form is added. The latter would be laid out by inscribing arcs of 0.25 and 1 tip chord radii within the tip plan form.

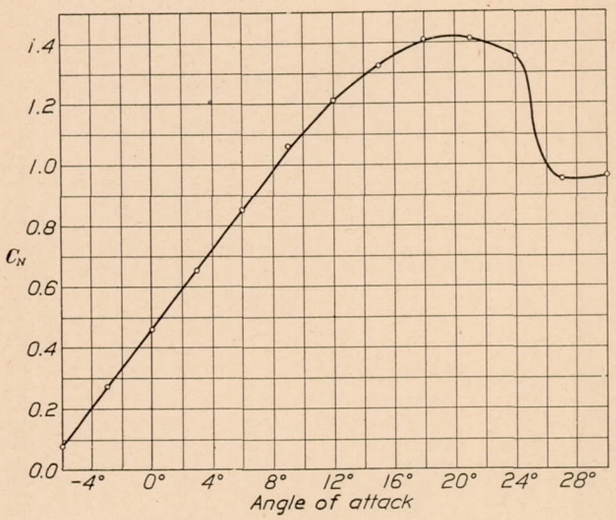

FIG. 24.—Total normal force—U. S. A. 35

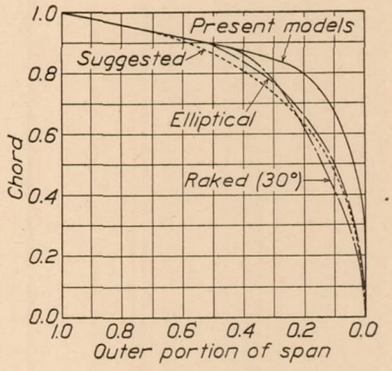

FIG. 25.—Wing tip forms

CONCLUSIONS

The distribution of pressure along the chords of these airfoils is very similar to that on thin airfoils; a greater portion of the surface experiences negative pressure at zero lift in thick sections than thin ones.

The distribution of load across the span of airfoils tapered as are the N. A. C. A. 81 and U. S. A. 35 and having a good form of wing tip is almost ideal from the aerodynamic point of view and is easily dealt with structurally.

While the tip form used on these wings would probably be easier to construct than one involving spars of unequal length, it is seen that a greater reduction of chord should be made close to the tip. Either the elliptical form or the shape suggested in the discussion is recommended.

To improve the distribution of load along the span, particularly at negative and small positive lifts, the wing should be twisted so that all sections will be at zero lift simultaneously.

The plan form used in the U. S. A. 27 C modified seems to have no apparent advantage, either structure or aerodynamic, over the straight tapered wings; in fact, it seems inferior from every point of view.

TABLE 1.—*Wing Section Ordinates in Per Cent of Chord; Stations in Per Cent of Chord from L. E.*

ROOT SECTION ORDINATES

Station	N. A. C. A. 81		U. S. A. 27 C modified		U. S. A. 35	
	U.	L.	U.	L.	U.	L.
0	+2.00	+2.00	+9.21	+9.21	+4.33	+4.33
1.25	4.50	−0.27	11.80	7.60	8.09	1.62
2.5	5.75	−0.90	13.32	7.03	9.58	0.96
5	7.80	−1.67	15.80	6.51	11.83	0.42
7.5	9.60	−2.33	17.45	6.02	13.58	0.22
10	11.07	−3.00	18.88	5.64	14.88	0.10
15	13.08	−4.13	20.68	5.05	16.60	0.00
20	14.33	−5.03	21.61	4.77	17.72	0.08
30	15.73	−6.05	22.40	4.72	18.43	0.25
40	15.73	−6.05	21.90	5.07	17.86	0.44
50	14.85	−5.70	20.85	5.48	16.16	0.60
60	13.15	−5.00	19.28	5.87	13.91	0.67
70	10.95	−4.05	17.40	6.25	11.12	0.65
80	8.40	−2.90	14.96	6.67	7.88	0.55
90	5.50	−1.50	11.65	7.10	4.33	0.32
95	3.95	−0.75	9.80	7.30	2.39	0.19
100	1.15	+1.15	7.75	7.75	0.22	0.22

L. E. R=2.06 R_U=5.45 R_L=3.24

T. E. Sharp. R=0.25 R =0.24

TIP SECTION ORDINATES

Station	N. A. C. A. 81		U. S. A. 27 C modified		U. S. A. 35	
	U.	L.	U.	L.	U.	L.
0	+0.50	+0.50	+11.86	+11.86	+2.76	+2.76
1.25	1.12	−0.06	13.05	11.15	5.15	1.03
2.5	1.44	−0.22	13.75	10.80	6.10	0.61
5	1.95	−0.42	15.00	10.54	7.53	0.27
7.5	2.40	−0.58	15.75	10.30	8.65	0.14
10	2.77	−0.75	16.38	10.12	9.47	0.06
15	3.27	−1.03	17.30	9.89	10.57	0.00
20	3.58	−1.26	17.80	9.72	11.28	0.05
30	3.94	−1.51	18.20	9.83	11.74	0.16
40	3.94	−1.51	18.00	10.00	11.37	0.28
50	3.71	−1.43	17.40	10.15	10.29	0.38
60	3.28	−1.25	16.70	10.30	8.85	0.43
70	2.73	−1.01	15.80	10.40	7.08	0.41
80	2.10	−0.72	14.50	10.58	5.02	0.35
90	1.37	−0.38	12.90	10.75	2.76	0.21
95	0.99	−0.19	12.02	10.86	1.52	0.12
100	0.29	+0.29	11.08	11.08	0.14	0.14

L. E. R=0.68 R_u=3.47 R_l=2.06

T. E. Sharp. R=0.11 R =0.15

Washed out 1.5°.

REFERENCES

Reference 1.—Bacon, David L., "The Distribution of Lift over Wing Tips and Ailerons." N. A. C. A. Technical Report No. 161, 1923.

Reference 2.—Norton, F. H. and Bacon, D. L., "Pressure Distribution over Thick Airfoils—Model Tests." N. A. C. A. Technical Report No. 150, 1922.

○

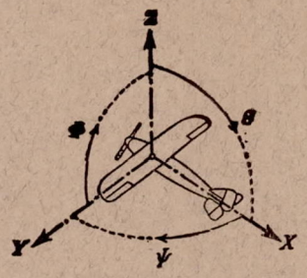

Positive directions of axes and angles (forces and moments) are shown by arrows

Axis		Force (parallel to axis) symbol	Moment about axis			Angle		Velocities	
Designation	Symbol		Designation	Symbol	Positive direction	Designation	Symbol	Linear (component along axis)	Angular
Longitudinal	X	X	rolling	L	$Y \longrightarrow Z$	roll	Φ	u	p
Lateral	Y	Y	pitching	M	$Z \longrightarrow X$	pitch	Θ	v	q
Normal	Z	Z	yawing	N	$X \longrightarrow Y$	yaw	Ψ	w	r

Absolute coefficients of moment

$$C_l = \frac{L}{qbS} \quad C_m = \frac{M}{qcS} \quad C_n = \frac{N}{qfS}$$

Angle of set of control surface (relative to neutral position), δ. (Indicate surface by proper subscript.)

4. PROPELLER SYMBOLS

Diameter, D

Pitch (a) Aerodynamic pitch, p_a
(b) Effective pitch, p_e
(c) Mean geometric pitch, p_g
(d) Virtual pitch, p_v
(e) Standard pitch, p_s

Pitch ratio, p/D

Inflow velocity, V'

Slipstream velocity, V_s

Thrust, T.

Torque, Q.

Power, P.

(If "coefficients" are introduced all units used must be consistent.)

Efficiency $\eta = T\,V/P$.

Revolutions per sec., n; per min., N.

Effective helix angle $\Phi = \tan^{-1}\left(\frac{V}{2\pi rn}\right)$

5. NUMERICAL RELATIONS

1 HP. = 76.04 kg/m/sec = 550 lb./ft./sec.
1 kg/m/sec = 0.01315 HP.
1 mi./hr. = 0.44704 m/sec
1 m/sec = 2.23693 mi./hr.

1 lb. = 0.4535924277 kg
1 kg = 2.2046224 lb.
1 mi. = 1609.35 m = 5280 ft.
1 m = 3.2808333 ft.